

Article

Raman Spectroscopy Enables Non-Invasive Identification of Mycotoxins *p. Fusarium* of Winter Wheat Seeds

Maksim N. Moskovskiy ^{1,*}, Aleksey V. Sibirev ¹, Anatoly A. Gulyaev ¹, Stanislav A. Gerasimenko ¹, Sergey I. Borzenko ¹, Maria M. Godyaeva ¹, Oleg V. Noy ², Egor I. Nagaev ³, Tatiana A. Matveeva ³, Ruslan M. Sarimov ³ and Alexander V. Simakin ³

¹ Federal Scientific Agroengineering Center VIM, 1st Institutskiy, Building 5, 109428 Moscow, Russia; sibirev2011@yandex.ru (A.V.S.); tomasss1086@mail.ru (A.A.G.); labintw@mail.ru (S.A.G.); Borzenko.serzh@yandex.ru (S.I.B.); airrune@yandex.ru (M.M.G.)

² L.L.C. Rostagroservice, Stadionnaya St., Building 7, 344012 Rostov-on-Don, Russia; oleg.neu@mail.ru

³ Prokhorov General Physics Institute of the Russian Academy of Sciences, Vavilova St. 38, 119991 Moscow, Russia; nagaev_e@kapella.gpi.ru (E.I.N.); pticek@yandex.ru (T.A.M.); rusa@kapella.gpi.ru (R.M.S.); avsimakin@gmail.com (A.V.S.)

* Correspondence: maxmoskovsky74@yandex.ru; Tel.: +7-903-401-05-02

Abstract: Identification of specific mycotoxins *p. Fusarium* contained in infected winter wheat seeds can be achieved by visually recognizing their distinctive phenotypic species. The visual identification (ID) of species is subjective and usually requires significant taxonomic knowledge. Methods for the determination of various types of mycotoxins of the *p. Fusarium* are laborious and require the use of chemical invasive research methods. In this research, we investigate the possibility of using Raman spectroscopy (RS) as a tag-free, non-invasive and non-destructive analytical method for the rapid and accurate identification of *p. Fusarium*. Varieties of the *r. Fusarium* can produce mycotoxins that directly affect the DNA, RNA and chemical structure of infected seeds. Analysis of spectra by RS methods and chemometric analysis allows the identification of healthy, infected and contaminated seeds of winter wheat with varieties of mycotoxins *p. Fusarium*. Raman seed analysis provides accurate identification of *p. Fusarium* in 96% of samples. In addition, we present data on the identification of carbohydrates, proteins, fiber and other nutrients contaminated with *p. Fusarium* seeds obtained using spectroscopic signatures. These results demonstrate that RS enables rapid, accurate and non-invasive screening of seed phytosanitary status.

Keywords: seeds of winter soft wheat; *p. Fusarium*; raman spectroscopy; fluorescence spectroscopy; identification of pathogenic microflora of seeds



Citation: Moskovskiy, M.N.; Sibirev, A.V.; Gulyaev, A.A.; Gerasimenko, S.A.; Borzenko, S.I.; Godyaeva, M.M.; Noy, O.V.; Nagaev, E.I.; Matveeva, T.A.; Sarimov, R.M.; et al. Raman Spectroscopy Enables Non-Invasive Identification of Mycotoxins *p. Fusarium* of Winter Wheat Seeds. *Photonics* **2021**, *8*, 587. <https://doi.org/10.3390/photonics8120587>

Received: 20 October 2021

Accepted: 11 December 2021

Published: 17 December 2021

Publisher's Note: MDPI stays neutral with regard to jurisdictional claims in published maps and institutional affiliations.



Copyright: © 2021 by the authors. Licensee MDPI, Basel, Switzerland. This article is an open access article distributed under the terms and conditions of the Creative Commons Attribution (CC BY) license (<https://creativecommons.org/licenses/by/4.0/>).

1. Introduction

Existing methods for detecting pathogenic microflora based on molecular biology, such as polymerase chain reaction (PCR) and enzyme-linked immunosorbent assay (ELISA). We destroy the sample in these methods and take a sufficient amount of time. It does not allow express diagnostics in the flow of seed material and directly in the field at the root of the plant.

Non-destructive (non-invasive) methods can be effectively used as reliable and accurate spectral instruments. Diagnostic of a grain crops includes several stages: first is detection of infected seeds without external signs of damage; the second is the detection of infected seeds at different stages of disease; the third is the identification of healthy seeds with the specification of the chemical composition and productive properties. The accuracy of these processes should be reached from 92 to 100 percentages. Raman spectroscopy (RS) is label-free, non-invasive and non-destructive analytical method that can be used to research the chemical composition of analyzed samples, to confirm the diagnosis of biotic and abiotic stresses in plants [1].

It is possible to diagnose with high accuracy several destructive fungal diseases of corn, wheat and sorghum with the help of a portable Raman spectrometer [2,3]. RS can be used for presymptomatic diagnosis of greening disease in citrus orange and grapefruit trees and pests inside cowpea seeds [4,5]. This method of research of non-contact diagnostics of biological effects can become tools in breeding, seed production and agronomy in order to increase the productivity of agriculture and control its phytocondition.

One of the most important grain crops cultivated in northern European countries is winter wheat (*Triticum aestivum* L.). The advantage of growing winter wheat is the ability to cultivate it in regions with different weather and climatic conditions, as well as a higher yield than the spring form. According to experts, the biological potential of winter varieties is 15–25% higher than that of the corresponding spring varieties. Most winter wheat varieties are soft. They are used for the manufacture of bakery products. Winter wheat flour contains a lot of gluten and it is actively used in the food industry.

However, growing winter wheat can affect the build-up of pathogens and affect future small-grain cash crops. The main disease of this culture is *fusarium* ear disease, grain damage by mycotoxins *p. Fusarium*. *Fusarium* head blight remains a problem in Europe and North America due to a limited set of fungicides (suppressive action), a narrow time window for use in the cultivation of cereals, a restriction on disease control by chemicals, resistance of pathogens and their subspecies variety, infection of plant residues (ear crops and corn), it is also possible to spread by fungi by spores at a distance within 5 km [6].

Varieties of *Fusarium* fungi (in particular *F. sporotrichioides*) release the T-2/IT-2 toxin (T-2 Toxin, C24H34O9) [7], suppress the synthesis of RNA and DNA. The toxin is resistant to high temperatures up to 280–300 °C. White crystalline substance with a molecular weight of 466, does not have fluorescence. In the EU countries, it is mandatory to analyze the content of fusariotoxins DON in grain products. The content of mycotoxin in a kilogram of grain or its processed products, in daily consumption per body weight (PHTDI—(1 µg/kg of body weight per day, for children 0.2 µg/kg of body weight per day) [8].

Due to the danger of grain contamination with mycotoxins, the main attention should be paid to the following species: *F. graminearum*, *F. sporotrichioides*, *F. langsethiae*, *F. poae*, *F. avenaceum* and *F. verticillioides*. The main mycotoxins that form the most common types of fungi *p. Fusarium*,—deoxynivalenol, nivalenol, T-2 and HT-2 toxins, moniliformin, fumonisins [9].

In this article, we have investigated the possibility of detecting fungi on wheat using Raman spectroscopy. In parallel, we used other methods of Near infrared analysis and Fluorescence spectroscopy to confirm the changes in wheat caused by the fungus. Previously, using Fluorescence spectroscopy, we showed the possibility of detecting rot on apples and potatoes [10]. We hope that it will be interesting for the reader to compare the capabilities of different non-invasive optical methods for the detection of plant diseases.

2. Materials and Methods

2.1. Materials

Winter wheat variety «Felicia» (Figure 1A) is a new mid-season variety of winter soft wheat, entered in 2019 in the State Register of Breeding Achievements of the Russian Federation in the Central Region. A sample is the winter wheat grain, variety «Felicia», harvest 2021. The spike is white, spinous, pyramidal in shape, of medium density. The kernal is red, semi-elongated, with a pronounced tuft. The keel tooth of the spikelet is of medium length, slightly curved; the shoulder is rounded, of medium width. Plant height is 75–85 cm. High adaptability to local climatic conditions of the new variety is manifested, first of all, in a stable yield over the years, the maximum reached 9.79 t/ha in 2017 [11].

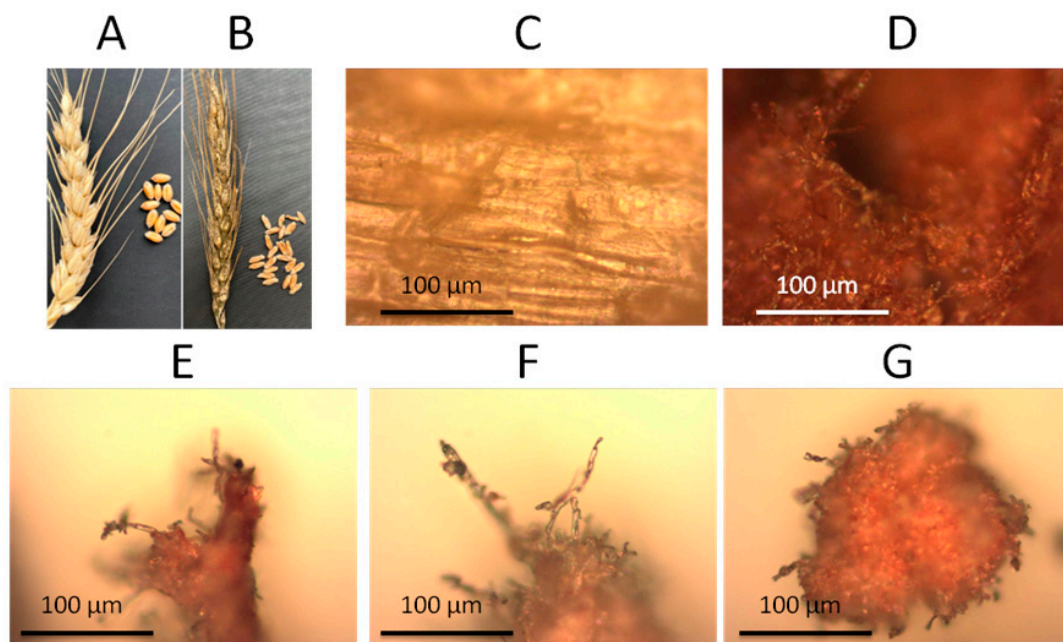


Figure 1. Healthy seeds of winter wheat cultivar «Felicia» (A). Infected *p. Fusarium* spike seeds winter wheat grade «Felicia» (B). Area and image of Raman measurement wheat seeds samples: image of the spectral measurement area on wheat seeds without *Fusarium* (C); image of the measurement area of spectra on wheat seeds infected with *Fusarium* (D), examples of scrapings of the samples with *Fusarium* (E–G).

2.2. Methods

Methods of the identifying grains infected with *p. Fusarium*. The degree of infection of a batch of winter wheat seeds, variety Felicia, harvest 2021, with *fusarium* was carried out in the Federal Service for Veterinary and Phytosanitary Surveillance of the Russian Federation FGBU “Center for Grain Quality Assessment” by a testing laboratory for determining the safety and quality of products, registration number ROSS RU 0001.21PT12. The method used was the “Method for determination of scabby kernels content” (Interstate Standard GOST 31646-2012). Acceptance rules and sampling methods GOST 13586.30-2015.

The main indicators of research: Infection of an average grain sample with mushrooms from the river. *Fusarium*—grain *fusarium* (FZ, %)—the ratio of the number of grains infected with fungi to the total number of analyzed grains; The sampling of samples (based on origin, culture, variety, etc.) is characterized by the proportion of samples with *fusarium* infection and indicators of grain infection in the sample: average, median and limits; The proportion (occurrence) of specimens with *fusarium* infection (%) is the ratio of the number of specimens in the sample with grains infected with fungi from the *r. Fusarium*, to the total number of analyzed samples; Average and median infestation (%) is calculated based on grain infestation (FZ) of all samples of the sample; The limits of infestation (%) show the minimum and maximum values of FZ in a sample of samples. Infection of grain with a certain type of river. *Fusarium* (%)—the ratio of the number of grains infected with this species to the total number of analyzed grains in the sample. The occurrence of a certain type of the river. *Fusarium* (%)—the number of samples in the sample with grains infected with this type of fungus, to the total number of analyzed samples; The share of a particular species in the complex of mushrooms of the *r. Fusarium* (%)—the ratio of the number of grains infected with a certain species of *p. Fusarium* to the number of grains infected with *p. Fusarium*. The sum of the shares of all types of the complex is always 100%.

The mass of the average sample is 2.0 ± 0.1 kg, the weight of the sample is not less than 25 g. According to this method, grains infected with *fusarium* were selected by their external sign: the shape and structure of the grain are feeble, have a strongly depressed groove; characteristics of the grain surface—stains and deposits are present; endosperm

structure—significant loss of vitreousness, endosperm—loose; the color of the embryo is the embryo on the cut of a dark color (brown), on the embryonic part and in the groove there is a light and light gray coating of the fungus. To assess micromorphological signs, agar media with a low carbohydrate content are used, on which the fungus forms a creeping, poorly developed, cobweb, colorless mycelium, the morphological features of which (size, shape of conidiophores, micro and macroconidia, chlamydospores, as well as methods of their formation) easily taken into account in situ [9]. *Fusarium* is not visible with a weak lesion of the mycelium, which are located in the shells of the grain. When the pathogen passes into the aleurone layer and the germ of the grain, the grain density deforms, their surface becomes deformed with the squeezing out of the furrow and the appearance of a pink tint.

Additionally, the method of thin layer chromatography (TLC) was used, the GC102AF device was a gas chromatograph with a FID TCD detector, for the detection of the T-2 toxin, by fluorescence in a long-wavelength UV light (365 nm) after treatment with an alcoholic solution of sulfuric acid followed by heating at 100–105 °C. The method can detect up to 100 ng of T-2 toxin in a stain of infected grain.

In accordance with the protocol No. 9710 dated 26 May 2021, on the basis of laboratory tests, it was established that a batch of winter wheat varieties “Felicia” weighing 2.0 kg with *Fusarium* 75.6% were infested; 59.4 ng of T-2 toxin was found in the grain contamination spot.

Raman spectroscopy. The Raman spectra were recorded on a Senterra spectrometer equipped with a CCD detector (Andor, IDUS), a laser with a wavelength of 785 nm, a diffraction grating of 400 lines/mm, an Olympus BX 51 microscope, and a motorized stage. We have chosen the following experimental conditions: Geometry of illumination of the sample—“reflection at 180°”, Objective—20×, Power of laser radiation—for the 785 nm line—20 mW. The accumulation time for the 785 nm line is 20 s.

Fluorescence spectroscopy. The fluorescence of healthy and *p. Fusarium* infected seeds was studied on a FP-8300 Spectrofluorometer (Jasco, Halifax, Canada). In total, 8 independent measurements of healthy and infected seeds were carried out. The measurements were carried out in a special cell for free-flowing samples (Figure 2D). The excitation bandwidth (20 nm) was made as large as possible in order to reduce the influence of the geometry of the arrangement of the seeds. The rest of the parameters were selected in such a way that the peaks of the maxima corresponded to approximately 30–40% of the instrument’s sensitivity. Emission bandwidth 1 nm, Response 50 ms, PMT voltage 500 V.

Near infrared analysis. Analysis in the near infrared region was carried out using Foss-NIRS-DS2500 (Foss, Hillerod, Denmark). The assay measured the percentage of protein, water, fat, cellulose, ash and starch in healthy and infected grains. Evaluation was carried out eight times with an average of five grains.

Real-time PCR. Primer specific for these pathogen was used to identify *Fusarium graminearum* in the respective samples (F-5′-GTTGATGGGTAAAAGTGTG-3′; R-5′-CTCTCA TATACCCTCCG-3′, Intergenic Spacer of rDNA (IGS region)) [12]. Primer was synthesized at the QuantStudio™ 5 Real-Time PCR System (Thermo Fisher, Waltham, MA, USA). The reaction mixture was prepared by mixing 5 µL of the ready-to-use qPCRmix-HS SYBR mixture (Evrogen, Russia) with a pair of target primers (1 µL each), 1 µL of the template DNA solution (1.28×10^2 ng/mL) and Milli-Q water to a volume of 25 µL. The real-time PCR reaction was performed in an O-DTLITE 4S1 amplifier (DNA technology, Russia). Fluorescence intensity measurements were performed at the end of the 72 °C cycle. Ct values, standard curves and corresponding correlation coefficients (R^2) were automatically obtained using Sequence Detection System v.1.2 software by interpolating Ct values against decimal logarithms of the original DNA concentrations. As a negative control, 2 µL of Milli-Q water was added to the reaction mixture instead of the DNA template. Three independent measurements were performed for each variant [13].

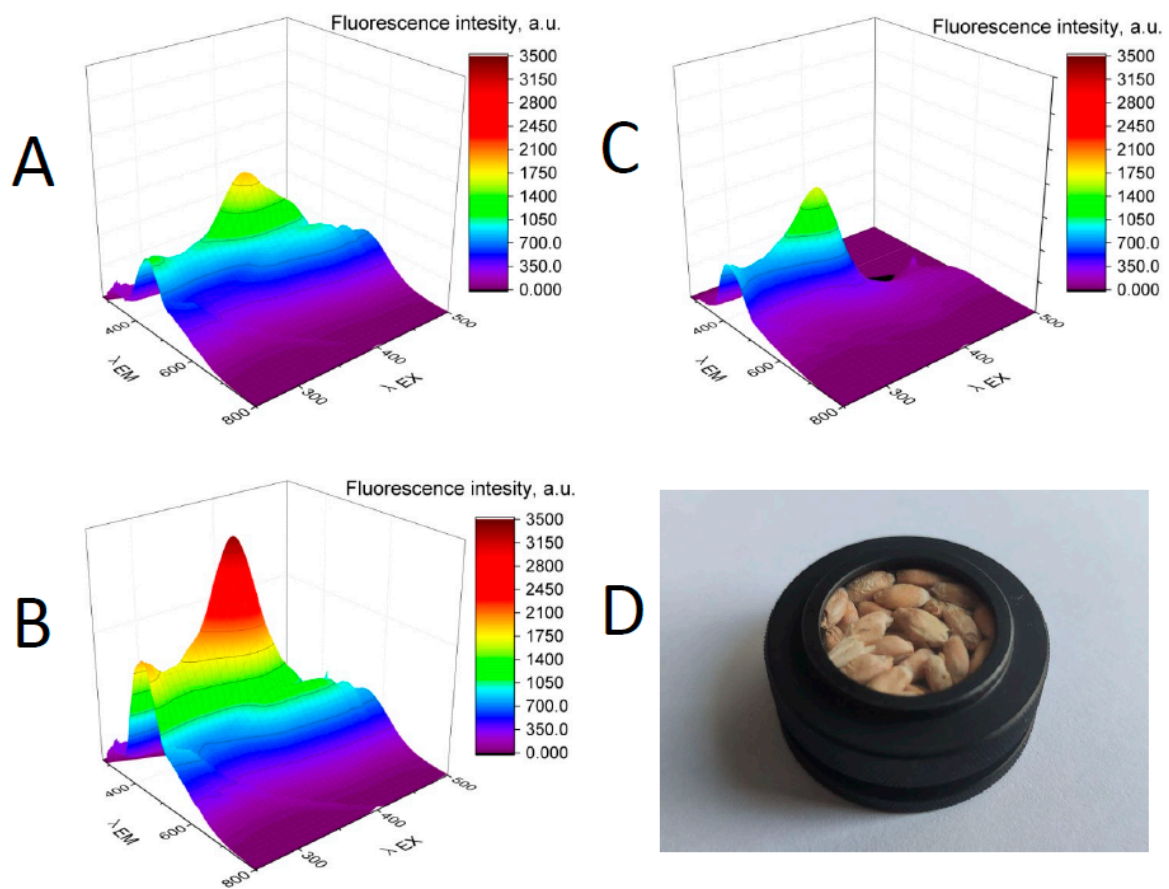


Figure 2. Fluorescence spectrum of healthy seeds (A), diseased of *p. Fusarium* (B) seeds and differential fluorescence spectrum (C). Data are presented as means for $n = 8$ samples. The measurement was carried out in a special cell for powder samples (D).

Statistical data analysis. Statistical analysis was performed using GraphPad Prism software (Version 8.0.1). The comparison of the average parameters in the method for healthy and infected *p. Fusarium* wheat was performed using the t-test. Correction for repeated measurements was made using the FDR test. Differences were considered significant at $p < 0.05$.

3. Results

Detection of Pathogens and Assessment of the Degree of Contamination of Samples. The infection was verified by RT-PCR. In samples of wheat (+), the DNA of *F. graminearum* (Ct ~13) was identified. In control samples (−), DNA of pathogen was not detected. In each variant of the experiment, three biological samples were analyzed. For each sample, 8 measurements were performed, the results of which were averaged. The proportion of affected seeds was more than 90%.

Figure 3 shows the Raman spectra of samples of *Fusarium graminearum*, obtained by excitation with a laser with a wavelength of 785 nm. It is shown that the spectrum of the pathogen *Fusarium graminearum* is quite characteristic. It is shown that the shape of the spectrum is significantly influenced by the water cut of the sample. In a sample containing about 10% water, water lines are present, for example, a strong line near 3200 cm^{-1} .

Figure 4 shows non-standardized spectra of control and infected seeds. It was shown that the spectra of infected and control seeds contain a fairly close and uniform set of maxima and minima. At the same time, the spectra of infected and control seeds have significant differences. A typical Raman spectrum of a protein exhibits a peptide bond carbonyl vibration at 1628 cm^{-1} known as the amide I band [14]. We observed a distinct

peak at about 1658 cm^{-1} in the spectra of *Fusarium*-infected maize kernels, which indicates that the growth of this pathogen is closely related to a change in the protein concentration in wheat grains. Vibrational bands around 1530 cm^{-1} originate from plane vibrations of $-\text{C}=\text{C}-$ and can be attributed to carotenoids (Table 1) [15]. The longer chain polyenes in these molecules show blue-shifted vibrational bands, while shorter-chain polyenes have redshift bands. However, in a more detailed study of the spectra, one should pay attention to the regions that differ both in the presence/absence of bands and in the change in the position of the vibration maxima in the spectrum.

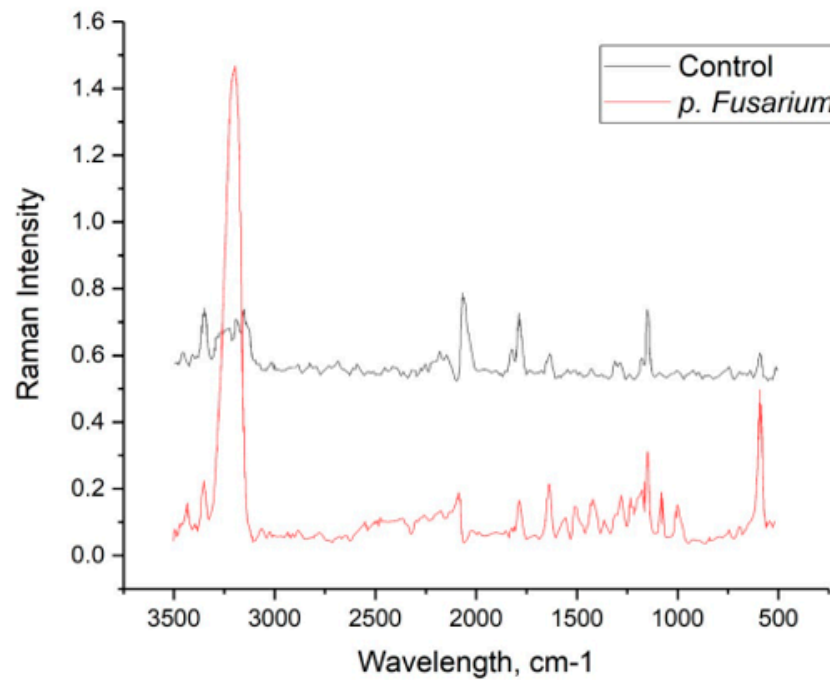


Figure 3. Raman spectra of *Fusarium graminearum* samples under normal conditions (red line) and after vacuum drying (black line).

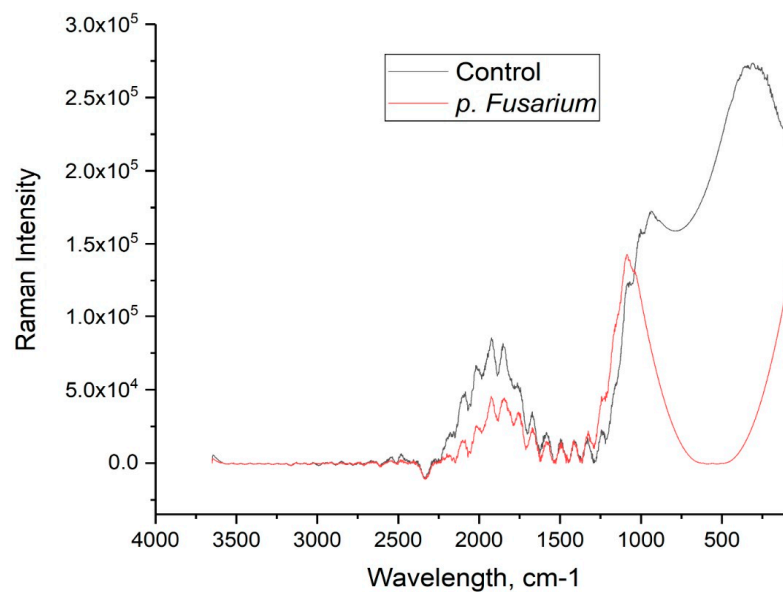


Figure 4. Raman spectra of seed samples of wheat infected and not infected with *Fusarium*. Data are presented as means for $n = 4$ samples.

Table 1. Matching vibrational bands.

Band (cm ⁻¹)	Vibrational Mode	Assignment
479.04–481.42	Deformations CCO and CCC; Associated with deformations of the skeleton of the glycosidic ring δ (C–C–C) + τ (C–O) notching C–C–C and bending C–O out of plane (CCO and CCC deformations; Related to glycosidic ring skeletal deformations δ (C–C–C) + τ (C–O) scissoring of C–C–C and out-of-plane bending of C–O)	Quantitative content of amylase [15,16]. Raman band at 480 cm ⁻¹ , related to the ring vibration of starches [15,16].
864	δ (C–C–H) + δ (C–O–C) glycosidic bond; anomeric region	Starch (range of carbohydrates 410–1259 cm ⁻¹) [1]
938	δ (C–O–C) + δ (C–O–H) + ν (C–O) α -1,4 glycosidic linkages	Starch (range of carbohydrates 410–1259 cm ⁻¹) [1]
1029–1031	In-plane CH ₃ rocking of polyene aromatic ring of phenylalanine	Cellulose, phenylpropanoids [17]
1126	ν (C–O) + ν (C–C) + δ (C–O–H)	Carotenoids [18]
1152	ν (C–O–C), ν (C–C) in glycosidic linkage, asymmetric ring breath	Starch (range of carbohydrates 410–1259 cm ⁻¹) [1]
1463–1458	δ (CH) + δ (CH ₂) + δ (C–O–H) CH, CH ₂ , and COH deformations	Carbohydrates [19]
1597–1504		Carbohydrates [16]
		Carotenoids [3]

The spectral region in the 3200–2700 cm⁻¹ range, which is responsible for the vibrations of bonds in the OH and NH functional groups. There is a significant difference in fluctuations in this area, which may be due to differences in the chemical composition of the cell wall of fungi, which includes fusarium and the cell wall of higher plants (wheat).

A detailed research of the Raman spectrum in the range of 400–1700 cm⁻¹ also indicates some differences, apparently associated with the presence of a pathogenic microorganism on the sample.

In all spectra of winter wheat seeds, two vibrational bands with centers at 1597 cm⁻¹ and 1504 cm⁻¹ were observed. In the spectrum of healthy winter wheat seeds, carotenoids showed an intense peak at 1597 cm⁻¹. In winter wheat seeds infected with pathogenic microflora of the genus *r. Fusarium* infected with pathogens, except for the peak at 1504 cm⁻¹ was more intense than the peak at 1597 cm⁻¹. This suggests that the growth of these pathogens on winter wheat seeds may be associated with degradation and fragmentation of host carotenoids [19]. Alternatively, it is possible that these pathogens produce specific short-chain carotenoids.

According to the reference analysis, differences in spectral information obtained by Raman scattering from samples not subjected to sample preparation, fluctuations in these areas may indicate the presence of microflora on a sample infected with fusarium.

Carbohydrates, including monomeric sugars and starch, are the main components of winter wheat seeds [20]. Sugars, mainly in the form of sucrose, are concentrated in the germ, where their content in wheat is over 20%. In general, sugar grains contain an average of 2–3%. Almost all starch is found in the endosperm of wheat seeds. In case of disease with pathogenic microflora, the endosperm of seeds is most affected. In case of disease with pathogenic microflora, the endosperm of seeds is most affected. Consequently, most of the observed vibrational bands originate from these molecules. The vibrational bands at 1126, 938 and 864 cm⁻¹ are associated with the C–O–C vibration, which is typical for starch.

Analysis in the near infrared shows that the infected seeds have increased protein, fat, cellulose and decreased water and starch (Tables 2 and 3). These changes are small, from 0.3% to 2.6%, but statistically significant. In addition, the SD for all measured parameters is more (sometimes twice) that for infected seeds.

Figure 2 shows the fluorescence spectra of healthy specimens (Figure 2A) and specimens infected with *p. Fusarium* (Figure 2B) and the differential spectrum (Figure 2C). It can be seen from the figure that the seeds infected with the *p. Fusarium* have a fluorescence peak twice as high as that of the control seeds. In addition, the fluorescence peak is shifted. The maximum of the control peak is in the region of $\lambda_{Ex} = 370$ nm for excitation and $\lambda_{Em} = 456$ nm for emission, while the infected seeds $\lambda_{Ex} = 364$ nm and $\lambda_{Em} = 439$ respec-

tively. The maximum of the differential peak is shifted to shorter wavelengths $\lambda_{Ex} = 360$ $\lambda_{Em} = 427$ (Figure 4).

Table 2. Near infrared analysis of the percentage of basic substances in healthy wheat seeds.

Object	Protein, %	Water, %	Fat, %	Cellulose, %	Ash, %	Starch, %
Sample 1	10.16	11.97	1.56	2.06	1.42	60.30
Sample 2	11.29	12.35	1.43	2.2	1.39	59.88
Sample 3	10.55	12.26	1.49	1.84	1.30	60.67
Sample 4	11.19	11.95	1.59	2.01	1.59	59.19
Sample 5	11.54	12.04	1.42	2.15	1.52	60.25
Sample 6	10.30	12.18	1.41	2.05	1.43	61.19
Sample 7	11.45	12.16	1.44	2.09	1.41	61.49
Sample 8	10.72	11.94	1.44	1.88	1.49	60.68
Mean	10.84	12.11	1.47	2.03	1.45	60.38
SD	0.536	0.154	0.068	0.125	0.088	0.727

Table 3. Near infrared analysis of the percentage of basic substances in infected *p. Fusarium* spike wheat seeds.

Object	Protein, %	Water, %	Fat, %	Cellulose, %	Ash, %	Starch, %
Sample 1	11.54	11.25	1.61	2.39	1.64	58.34
Sample 2	12.74	11.08	1.70	2.58	1.77	57.83
Sample 3	12.48	11.12	1.77	2.15	1.66	60.59
Sample 4	11.75	10.44	1.82	2.41	1.76	59.80
Sample 5	11.19	10.89	1.80	2.2	1.74	57.98
Sample 6	11.84	11.00	1.80	2.51	1.8	56.60
Sample 7	12.79	11.19	1.68	2.64	1.72	57.80
Sample 8	11.10	10.53	2.09	2.50	2.23	53.70
Mean	11.91 **	10.95 ***	1.77 ***	2.44 ***	1.77 ***	57.82 **
SD	0.668	0.302	0.144	0.174	0.186	2.084

t-test *p*-level ** < 0.01, *** < 0.001.

4. Discussion

According to the fluorescence data, the appearance of additional fluorescence in the spectra of *p. Fusarium* infected seeds in the short-wavelength region is clearly visible. The fungi can fluoresce themselves especially since they are located on the surface of the seeds. The increase in fluorescence can be due to several reasons. Firstly, this is possible due to the proteins that contain the aromatic amino acids Phe, Tyr and Trp (this is the area $\lambda_{Ex} \sim 220\text{--}310$ and $\lambda_{Em} \sim 320\text{--}400$) [20]. The fact that proteins can make such a significant contribution is confirmed by the data of the infrared spectrum analyzer. This showed more than a percentage increase in protein content in grain samples containing fungus (Tables 2 and 3). In addition, the fungus is localized on the surface of the seed, which can be seen from the photographs obtained with a microscope (Figure 1).

The second reason fungi and their spores themselves have emission peaks in the region of 400–500 nm when excited in the range of 250–350 nm [21–23]. This fluorescence can be ascribed to the reduced form of the nicotinamide-adenine dinucleotide phosphate (NADP), which is known to emit fluorescence in blue region with a maximum ~440–465 nm [24]. The third possible cause is the fluorescence of fungal pigments [25], metabolites [26] and toxins [27]. The identification of toxins is especially important in the context of their possible consumption with food and entering the human body.

It is characteristic that blue-green fluorescence in plants and grains is mainly associated with phenol compounds [28], which are usually localized in the cell wall [29,30] and perform mainly antioxidant and protective functions, including against fungal diseases [31].

Pathogenic activity of mycotoxins influences the processes of starch degradation and their conversion into monomeric sugars and polymeric hydrocarbons. Changes in vibrational bands at 1126, 938 and 864 cm in healthy and infected *r. Fusarium*, winter wheat seeds allow identification of their infestation.

The proposed non-invasive and non-destructive spectroscopic method for the detection and identification of pathogenic microflora of winter wheat seeds is effective for phytosanitary control of fields and the yield of grain crops, for the subsequent detection of mycotoxins, which form the most common types of fungi of the *r. Fusarium*,—deoxynivalenol, nivalenol, T-2 and HT-2 toxins, moniliformin, fumonisin, as well as mycotoxins of the species: *F. graminearum*, *F. sporotrichioides*, *F. langsethiae*, *F. poae*, *F. avenaceum* and *F. verticillioides*.

5. Conclusions

Subsequent research by the RS method of carotenoids, in particular, changes in their structures and quantitative components in the spectral range of 1400–1600 cm⁻¹, may be promising for the identification of pathogenic microflora of grain crops. This will lead to a million-fold increase in their signals, allowing for a better understanding of the structural changes in the carotenoid component of maize. associated with fungal infections. Also promising is the study of ring vibrations of cereal starches in the range of 480–1259 cm⁻¹ to determine the identification markers of infection by pathogenic microflora of cereal seeds.

Author Contributions: Conceptualization—M.N.M. and A.V.S. (Aleksey V. Sibirev); methodology—A.V.S. (Alexander V. Simakin); investigation—Raman spectroscopy—M.M.G. and S.I.B.; fluorescence spectroscopy—R.M.S.; real-time PCR—E.I.N. and T.A.M.; Near infrared analysis—M.M.G.; resources—S.A.G. and S.I.B.; writing original draft preparation—A.A.G. and O.V.N.; writing review and editing—R.M.S. and A.V.S. (Aleksey V. Sibirev); supervision—M.N.M. All authors have read and agreed to the published version of the manuscript.

Funding: This work was supported by a grant of the Ministry of Science and Higher Education of the Russian Federation for large scientific projects in priority areas of scientific and technological development (grant number 075-15-2020-774).

Institutional Review Board Statement: Not applicable.

Informed Consent Statement: Not applicable.

Data Availability Statement: Not applicable.

Conflicts of Interest: The authors declare no conflict of interest.

References

1. Farber, C.; Islam, A.S.M.F.; Septiningsih, E.M.; Thomson, M.J.; Kurouski, D. Non-Invasive Identification of Nutrient Components in Grain. *Molecules* **2021**, *26*, 3124. [[CrossRef](#)]
2. Egging, V.; Nguyen, J.; Kurouski, D. Detection and Identification of Fungal Infections in Intact Wheat and Sorghum Grain Using a Hand-Held Raman Spectrometer. *Anal. Chem.* **2018**, *90*, 8616–8621. [[CrossRef](#)]
3. Farber, C.; Kurouski, D. Detection and Identification of Plant Pathogens on Maize Kernels with a Hand-Held Raman Spectrometer. *Anal. Chem.* **2018**, *90*, 3009–3012. [[CrossRef](#)] [[PubMed](#)]
4. Sanchez, L.; Farber, C.; Lei, J.X.; Zhu-Salzman, K.; Kurouski, D. Noninvasive and Nondestructive Detection of Cowpea Bruchid within Cowpea Seeds with a Hand-Held Raman Spectrometer. *Anal. Chem.* **2019**, *91*, 1733–1737. [[CrossRef](#)] [[PubMed](#)]
5. Sanchez, L.; Pant, S.; Xing, Z.L.; Mandadi, K.; Kurouski, D. Rapid and noninvasive diagnostics of Huanglongbing and nutrient deficits on citrus trees with a handheld Raman spectrometer. *Anal. Bioanal. Chem.* **2019**, *411*, 3125–3133. [[CrossRef](#)]
6. D'Angelo, D.L.; Bradley, C.A.; Ames, K.A.; Willyerd, K.T.; Madden, L.V.; Paul, P.A. Efficacy of Fungicide Applications during and After Anthesis against Fusarium Head Blight and Deoxynivalenol in Soft Red Winter Wheat. *Plant Dis.* **2014**, *98*, 1387–1397. [[CrossRef](#)]
7. Center for Disease Control and Prevention Federal Select Agent Program. Select Agent and Toxin List. 2017. Available online: www.selectagents.gov/sat/list.htm (accessed on 10 December 2021).

8. Commission Regulation EC. 2005. Available online: <https://eur-lex.europa.eu/legal-content/EN/ALL/?uri=CELEX%3A32005R2073> (accessed on 10 December 2021).
9. Gagkaeva, T.Y.; Gavrilova, O.P.; Levitin, M.M.; Novozhilov, K.V. Fusarium of grain crops. *Plant Prot. Quar.* **2011**, *5*.
10. Sarimov, R.M.; Lednev, V.N.; Sibirev, A.V.; Gudkov, S.V. The Use of Fluorescence Spectra for the Detection of Scab and Rot in Fruit and Vegetable Crops. *Front. Phys.* **2021**, *8*, 640887. [[CrossRef](#)]
11. Levakova, O.V.; Barkovskaya, T.A.; Bannikova, M.I. New variety of winter soft wheat Felicia. *Bull. Russ. Agric. Sci.* **2020**, *3*. [[CrossRef](#)]
12. Penkov, N.V.; Goltyaev, M.V.; Astashev, M.E.; Serov, D.A.; Moskovskiy, M.N.; Khort, D.O.; Gudkov, S.V. The Application of Terahertz Time-Domain Spectroscopy to Identification of Potato Late Blight and Fusariosis. *Pathogens* **2021**, *10*, 1336. [[CrossRef](#)] [[PubMed](#)]
13. Sharapov, M.G.; Novoselov, V.I.; Fesenko, E.E.; Bruskov, V.I.; Gudkov, S.V. The role of peroxiredoxin 6 in neutralization of X-ray mediated oxidative stress: Effects on gene expression, preservation of radiosensitive tissues and postradiation survival of animals. *Free Radic. Res.* **2017**, *51*, 148–166. [[CrossRef](#)]
14. Fellows, A.P.; Casford, M.T.L.; Davies, P.B. Spectral Analysis and Deconvolution of the Amide I Band of Proteins Presenting with High-Frequency Noise and Baseline Shifts. *Appl. Spectrosc.* **2020**, *74*, 597–615. [[CrossRef](#)] [[PubMed](#)]
15. Krimmer, M.; Farber, C.; Kurouski, D. Rapid and Noninvasive Typing and Assessment of Nutrient Content of Maize Kernels Using a Handheld Raman Spectrometer. *ACS Omega* **2019**, *4*, 16330–16335. [[CrossRef](#)]
16. Almeida, M.R.; Alves, R.S.; Nascimbem, L.; Stephani, R.; Poppi, R.J.; de Oliveira, L.F.C. Determination of amylose content in starch using Raman spectroscopy and multivariate calibration analysis. *Anal. Bioanal. Chem.* **2010**, *397*, 2693–2701. [[CrossRef](#)] [[PubMed](#)]
17. Edwards, H.G.M.; Farwell, D.W.; Webster, D. FT Raman microscopy of untreated natural plant fibres. *Spectrochim. Acta Part A-Mol. Biomol. Spectrosc.* **1997**, *53*, 2383–2392. [[CrossRef](#)]
18. Schulz, H.; Baranska, M.; Baranski, R. Potential of NIR-FT-Raman spectroscopy in natural carotenoid analysis. *Biopolymers* **2005**, *77*, 212–221. [[CrossRef](#)]
19. Wiercigroch, E.; Szafraniec, E.; Czamara, K.; Pacia, M.Z.; Majzner, K.; Kochan, K.; Kaczor, A.; Baranska, M.; Malek, K. Raman and infrared spectroscopy of carbohydrates: A review. *Spectrochim. Acta Part A-Mol. Biomol. Spectrosc.* **2017**, *185*, 317–335. [[CrossRef](#)] [[PubMed](#)]
20. Bortolotti, A.; Wong, Y.H.; Korsholm, S.S.; Bahring, N.H.B.; Bobone, S.; Tayyab, S.; van de Weert, M.; Stella, L. On the purported “backbone fluorescence” in protein three-dimensional fluorescence spectra. *RSC Adv.* **2016**, *6*, 112870–112876. [[CrossRef](#)]
21. Pan, Y.L.; Hill, S.C.; Pinnick, R.G.; House, J.M.; Flagan, R.C.; Chang, R.K. Dual-excitation-wavelength fluorescence spectra and elastic scattering for differentiation of single airborne pollen and fungal particles. *Atmos. Environ.* **2011**, *45*, 1555–1563. [[CrossRef](#)]
22. Raimondi, V.; Palombi, L.; Cecchi, G.; Lognoli, D.; Trambusti, M.; Gomoiu, I. Remote detection of laser-induced autofluorescence on pure cultures of fungal and bacterial strains and their analysis with multivariate techniques. *Opt. Commun.* **2007**, *273*, 219–225. [[CrossRef](#)]
23. Raimondi, V.; Agati, G.; Cecchi, G.; Gomoiu, I.; Lognoli, D.; Palombi, L. In vivo real-time recording of UV-induced changes in the autofluorescence of a melanin-containing fungus using a microspectrofluorimeter and a low-cost webcam. *Opt. Express* **2009**, *17*, 22735–22746. [[CrossRef](#)] [[PubMed](#)]
24. Konig, K.; Berns, M.W.; Tromberg, B.J. Time-resolved and steady-state fluorescence measurements of beta-nicotinamide adenine dinucleotide-alcohol dehydrogenase complex during UVA exposure. *J. Photochem. Photobiol. B-Biol.* **1997**, *37*, 91–95. [[CrossRef](#)]
25. Lagashetti, A.C.; Dufosse, L.; Singh, S.K.; Singh, P.N. Fungal Pigments and Their Prospects in Different Industries. *Microorganisms* **2019**, *7*, 604. [[CrossRef](#)] [[PubMed](#)]
26. Khundzhua, D.A.; Patsaeva, S.V.; Terekhova, V.A.; Yuzhakov, V.I. Spectral Characterization of Fungal Metabolites in Aqueous Medium with Humus Substances. *J. Spectrosc.* **2013**, *2013*, 538608. [[CrossRef](#)]
27. Fredlund, E.; Gidlund, A.; Pettersson, H.; Olsen, M.; Borjesson, T. Real-time PCR detection of Fusarium species in Swedish oats and correlation to T-2 and HT-2 toxin content. *World Mycotoxin J.* **2010**, *3*, 77–88. [[CrossRef](#)]
28. Lang, M.; Stober, F.; Lichtenthaler, H.K. Fluorescence emission-spectra of plant-leaves and plant constituents. *Radiat. Environ. Biophys.* **1991**, *30*, 333–347. [[CrossRef](#)]
29. Harris, P.J.; Hartley, R.D. Detection of bound ferulic acid in cell-walls of gramineae by ultraviolet fluorescence microscopy. *Nature* **1976**, *259*, 508–510. [[CrossRef](#)]
30. Lichtenthaler, H.K.; Schweiger, J. Cell wall bound ferulic acid, the major substance of the blue-green fluorescence emission of plants. *J. Plant Physiol.* **1998**, *152*, 272–282. [[CrossRef](#)]
31. Vermerris, W.; Nicholson, R. *Phenolic Compound Biochemistry*; Springer Science & Business Media: Berlin/Heidelberg, Germany, 2007.